Effects of DC electric fields on the combustion of a simplified multi-element injector

Paulo Roberto Salvador[1], Kunning Gabriel Xu[2]

The University of Alabama in Huntsville, Huntsville, AL 35899

Nomenclature

Φ	=	equivalence ratio
U	=	flow velocity, m/s
$\vec{E}$	=	electric field, V/m
∇	=	del operator
V	=	voltage, V
ε	=	electrical permittivity, F/m
D	=	electric flux density, C/m^2
ρ	=	free electric charge density, C/m^3

I.   Introduction

The ability to modify a flame's behavior with electric fields has been investigated since the 1800s when changes in heat and mass transfer were reported by Brande[1]. Over the years more elaborate and detailed studies[2–14] have given more insight into the characteristics of the interaction between a flame and electric fields and the mechanisms involved in this interaction. In the experiments conducted by Payne and Weinberg[15] and Lawton and Weinberg[16] the ionic wind body-force was attributed as the driving mechanism for the observed effects the electric field caused on a flame. The ionic wind body-force is an electro-hydrodynamic effect caused by electron-neutral and ion-neutral collisions, and the rate of these collisions influence the flame behavior, making it a momentum driven process. Electron-molecule collisions have only a small contribution to the ionic wind effect due to the small mass of electrons. These collisions are caused by the electric field creating an electric current between the electrodes that drives positive ions toward the cathode and negative ions and electrons toward the anode. The process of momentum transfer from these collisions is sustained for as long as a voltage difference between the electrodes exists.

The results of these studies have shown the ability of an electric field to increase flame stability by extension of its lower flammability limit and increased blowoff velocity[2–6,11], reduce CO and NO$_x$ emissions[13,14], and potentially suppress or modify different modes of thermoacoustic and thermodiffusive instabilities[10,12,17,18] at several different experimental conditions. Most of the experiments in the literature are conducted utilizing a single burner with a ring or grid electrode due to its simplicity for understanding the physics; however, real combustion devices such as rocket engines have multiple injectors and cylindrical combustor geometry. In this paper, we investigated the effects of an applied DC electric field on two burner configurations consisting of a single burner and a simplified multi-element burner inside a large cylindrical can electrode, both operating with a premixed methane-air flame at atmospheric conditions. The use of DC electric fields versus microwave, RF, or pulsed DC is due to the simplicity of steady DC and the ease of scaling with pressure[14].

This study compared the effects of an applied DC electric field on the lean flammability limit and blowoff velocity between a single burner and a multi-element burner configuration. The goal was to understand how the different element locations and the potential for flame interaction affect the electric field induced effects as a simplified, atmospheric analogy for liquid rocket engines injectors. Numerical simulations of the electric fields using finite element software were done to provide further insight into the physics.

II.   Experimental Setup

The experimental setup, shown in Figure 1, consisted of a manifold with 4 outlet ports from which four burners could be installed, a cylindrical chamber opened on both ends, and a DC high-voltage power supply with a maximum voltage of 10 kV and current limited at 10 mA. The manifold and burners were grounded and functioned as the cathode in the system, whereas the cylindrical chamber acted as the anode. Although not shown in Figure 1, a

---

[1] Graduate Research Assistant, Propulsion Research Center, 301 Sparkman Dr., Huntsville, AL 35899
[2] Assistant Professor, Mechanical and Aerospace Engineering, 301 Sparkman Dr., Huntsville, AL 35899

ring anode was also used for the single-burner test configuration. A rich ($\Phi = 1.16$), premixed methane-air mixture was fed into the manifold and burners, and the volumetric flow rate of each gas was controlled by a mass flow controller as depicted in Figure 1.

Previous studies[13,14,19] have reported the importance of electrode location for optimizing the electric field effects observed on a flame. Two different anodes were used to characterize the flame behavior in this work, a stainless steel cylinder and a copper ring. This choice of anodes alters the anode surface area and location with respect to the flame front. The larger surface area cylinder should generate a larger field potential gradient, for a given voltage, and thus a larger effect on the flame. The cylindrical chamber had inner and outer diameters of 162 mm and 168 mm, respectively, and was 154 mm tall. This anode geometry was chosen with the intent of emulating a simplified rocket engine combustion chamber. A copper ring with inner diameter of 152 mm was also used in a few of the tests in this study. Both cylinder and ring upper rims were 88 mm above the burner exit.
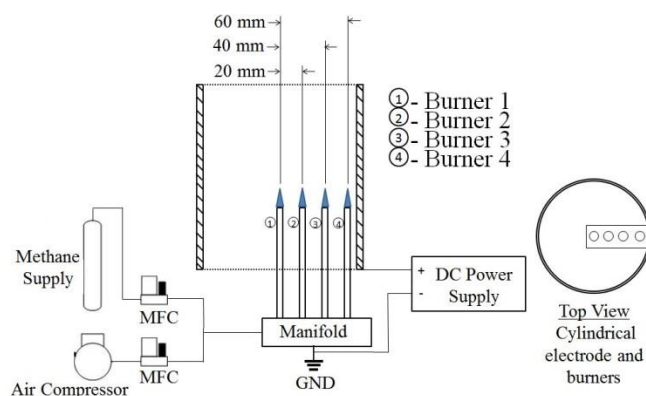

Figure 1. Experimental setup showing a simplified multi-element injection burner (grounded) and cylindrical chamber (anode).

The first configuration used a single burner 7 mm ID burner tube and investigated the electric field effect on the flame with the burner at three different radial locations: center, 40 mm, and 60 mm with both anodes. The field effect was quantified by measuring its effect on the flame blowoff velocity and lean flammability limit at various test conditions. Blowoff velocity tests were conducted by increasing both the air and fuel flow rate while maintaining $\Phi=1.16$. Flammability limit tests were conducted by decreasing fuel flow and increasing air flow while holding a constant total flow rate of 2.50 SLM. The second burner configuration used four burners installed 20 mm from each other as shown in Figure 1, where Burner 1 is the center burner and 4 is the outer burner at 60 mm. The blowoff test conditions (i.e., $\Phi = 1.16$) remained the same for the multiple burner tests, but the flow rate for the flammability limit tests was increased to a total of 10.00 SLM to provide roughly the same flow rate per burner as the single burner case. Results from this test were used to determine how the modified flames response in a multiple flame system would differ from the single burner case.

Numerical simulations using Finite Element Method Magnetics (FEMM) were done to model the electric field produced by different anodes and burner configurations. The simulations only focused on predicting the electric field behavior for the different configurations tested since the program is unable to simulate reaction chemistry. The presence of electrically charged flame plasma will alter the results from the simulations; however, the electric field maps should provide some insight into the different behaviors observed.

III.   Experimental Results

A.   Lean Flammability Limit Extension

A fuel-air mixture only ignites, and is sustained, within a specific mixture ratio between the lower and upper limits of flammability[20]. In addition to the physicochemical properties of the mixture, flammability limits also depend on experimental setup factors such as heat loss to the burner and surroundings[21]. To minimize the effects of

these losses, the study was carried out on the same apparatus and at constant volumetric flow rates throughout its entirety.

Single Burner Configuration

The lean flammability limit was determined at three radial positions using both anode geometries to investigate the effects of burner position, electrode gap and anode surface area on the flame. Figure 2 shows an extension of the flame lean limit of flammability with increasing bias voltage with both anode geometries.
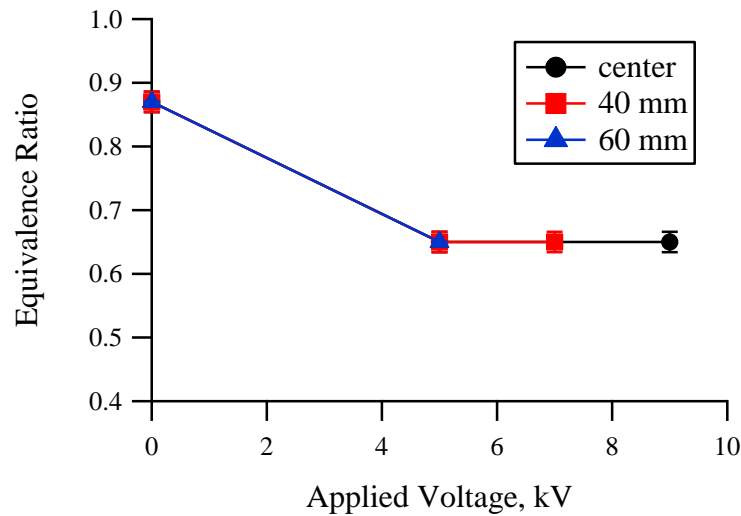
a) cylinder
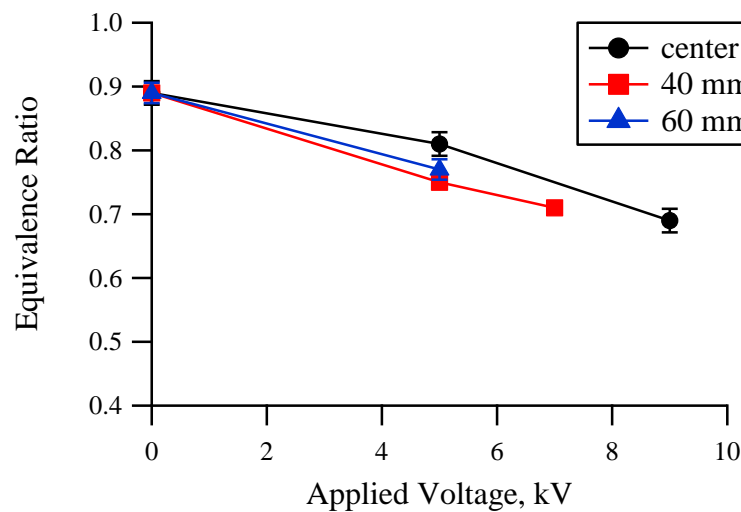
b) ring

Figure 2. Extension of the lower limit of flammability for a premixed methane-air flame using a) cylindrical chamber and b) ring anodes.

The lean limit equivalence ratio for the cylindrical anode at all three locations was extended from 0.87 at 0 V to 0.65 at 5 kV, independent of the burner location (Fig. 2a). Further increase in the bias voltage resulted in no further extension of the lean limit which indicates the existence of a critical limit to the electric field effect for the

conditions investigated. Higher voltages were not possible due to arcing between the electrodes. The ring anode configuration showed a smaller extension of the lean limit at 5 kV than the cylinder, and it was also sensitive to the radial location of the burner. Flame equivalence ratio for the center burner decreased from 0.89 at 0 V to 0.80 at 5 kV. At 9 kV the equivalence ratio decreased to 0.68. The 40 and 60 mm burner cases showed a more significant decrease at 5 kV, from 0.89 to 0.75 and 0.77, respectively. Table 1 provides a summary of the flammability limit results obtained for a single burner at the three radial locations as a function of the applied voltage and anode geometry.

Table 1 Single burner flammability results as a function of burner location and applied voltage.

Bias Voltage, kV	Cylindrical Chamber			Ring		
	Φ_{center}	Φ_{40mm}	Φ_{60mm}	Φ_{center}	Φ_{40mm}	Φ_{60mm}
0	0.87	0.87	0.87	0.89	0.89	0.89
5	0.65	0.65	0.65	0.80	0.75	0.77
7	-	0.65	-	-	0.71	-
9	0.65	-	-	0.68	-	-

Based on the results of the cylindrical and ring anodes, it is clear that the anode surface area is a factor in the flame response. The cylindrical anode produced a stronger effect on the flame, in this case a larger extension in the lean limit, e.g. the cylinder reached $\Phi = 0.65$ at 5 kV instead of 9 kV. Since bias voltage is directly proportional to electric power, this indicates the cylinder is more efficient to extend the lean flammability limit.

Multiple Burners Configuration

Tests with the multiple burner configuration was conducted only with the cylinder anode since it was shown to cause larger extension of flame lean limit for a given voltage. This burner configuration was used to investigate how a combination of increased cathode surface area and flame-to-flame interaction would change the flame response and thus its lean limit. Since all four burners were fed from the same manifold, the overall equivalence ratio to the manifold was continually decreased until all the flames disappeared. The equivalence ratio when each flame extinguished was recorded as the lean limit for that burner. The results seen in Figure 3 shows the 4 burners had different lean limits at a given voltage and larger extensions were observed for burners closer to the anode wall.
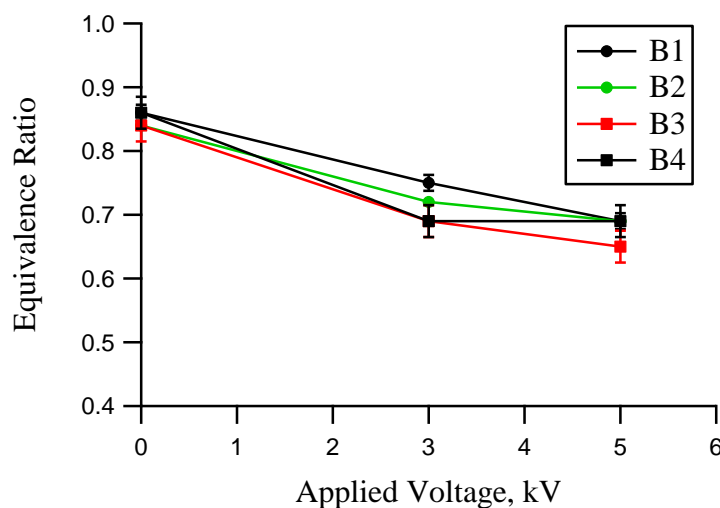

Figure 3. Extension of the lean limit of flammability for a premixed methane-air flame using a multi-element burner and cylinder anode. B1-4 are burners 1-4 from center to 60 mm as shown in Figure 1.

The graph shows the lean limit varied for each burner. Indeed, as the equivalence ratio was decreased, the burner flames went out at different conditions. The tests were repeated at least three times and each time showed the same pattern. Burner 1, 2, and 4 had an extension from $\Phi=0.86$ at 0 kV to 0.69 at 5 kV whereas burner 3 had an extension down to $\Phi=0.65$ for the same bias voltage. The converging of the lean limit equivalence ratio to 0.69 at 5 kV for burner 1, 2, and 4 indicates a critical limit of the electric field effect for the conditions investigated, as it was seen for the single burner configuration.

B.   Blowoff Velocity

Flame stability is achieved by matching of the local flame speed and local flow velocity. Blowoff and liftoff conditions occur when the flow velocity exceeds the flame speed, causing the flame to detach from the burner rim and eventually extinguish. Flame speed is primarily a chemical property dependent on the mixture ratio, pressure, and temperature.

Single Burner Configuration

Similar to the flammability limit experiment, the blowoff velocity for the single burner configuration was determined at three burner locations (center, 40, and 60 mm from the center) with both anode geometries (cylinder and ring). As expected, an increase in flame blowoff velocity was achieved when the flame is subject to an electric field. In contrast to the cylinder anode results for lean flammability limit extension, the blowoff velocity changed with different radial location, as shown in Fig. 4. With the cylindrical anode, the maximum blowoff velocity measured was roughly equal, ~10 m/s, at all three burner locations, but at different voltages (Fig. 4a). The closer to the wall, the lower the voltage needed. The ring anode follows the same trend that the 40 and 60 mm locations saw a greater increase in blowoff velocity for a given voltage. It is likely the blowoff velocity could have been increased even further with higher voltages, however the experiment was limited by the 10 kV power supply and arcing between the electrodes for the 40 and 60 mm locations. Although both anodes increased the blowoff velocity, the cylinder anode achieved the largest increase for a given voltage.
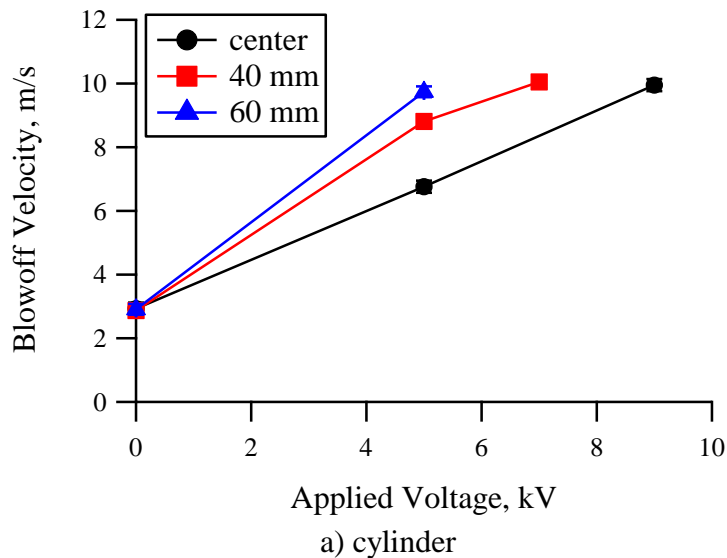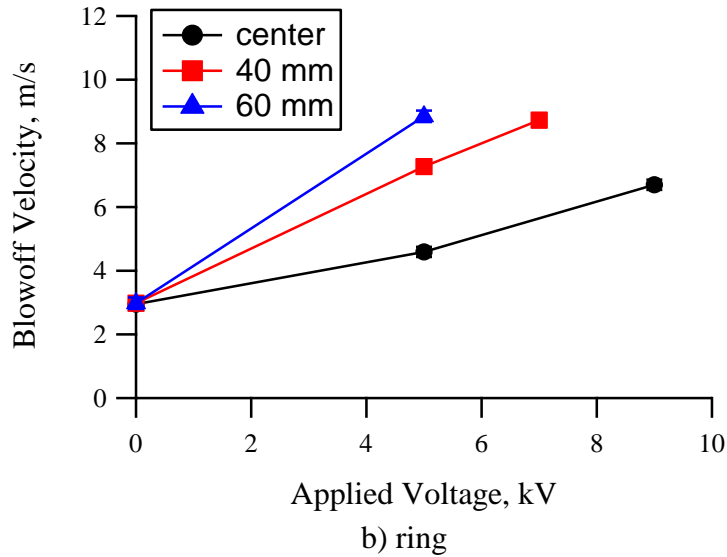

a) cylinder

b) ring

Fig. 4 Blowoff characteristics for a premixed methane-air flame with electric field interaction on a a) cylinder and b) ring anodes.

Table 2 summarizes the blowoff results for the single burner configuration. A direct comparison shows that the cylinder anode causes a stronger flame response than the ring anode, similar to the lean flammability limit. Thus, again, indicates a dependency on burner location and anode surface area. The cylinder had a greater increase in blowoff velocity than the ring at all experimental conditions.

Table 2 Single burner blowoff velocity results as a function of burner location and applied voltage.

Bias Voltage, kV	Cylindrical Chamber			Ring		
	U_{center}	U_{40mm}	U_{60mm}	U_{center}	U_{40mm}	U_{60mm}
0	2.93	2.87	2.91	2.95	2.98	2.98
5	6.76	8.81	9.74	4.59	7.27	8.85
7	-	10.05	-	-	8.73	-
9	9.95	-	-	6.70	-	-

Multiple Burners Configuration

In the multi-element burner tests, the blowoff velocity was measured with the assumption that the total flow rate into the manifold was evenly distributed to all four burners. For these tests, only the cylinder anode was utilized. Figure 5 shows the blowoff velocity is a linear function of the applied voltage, and the same for all burners. Visually, all four burners appear to blowoff at the same time once the flow rate is increased past the limit. This is a significant departure from the four burner lean limit results and the single burner blowoff results. Both previously indicated the four burners had different responses due to their radial location. This indicates that something is affecting or linking the behavior of each individual burner so they behave as a single unit, at least for the blowoff velocity tests.

The maximum blowoff velocity is also noticeably higher than the single burner case. The presence of multiple flames seems to sustain each other by increasing the total heat release inside of the cylinder anode. This behavior is evident when comparing both configurations at the 0 kV case. The blowoff velocity occurred at ~2.90 m/s for the center, 40, and 60 mm burner locations in the single burner case, whereas for the multi-element burner this velocity was at ~5.80 m/s.
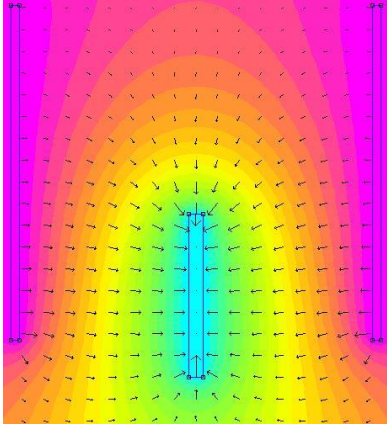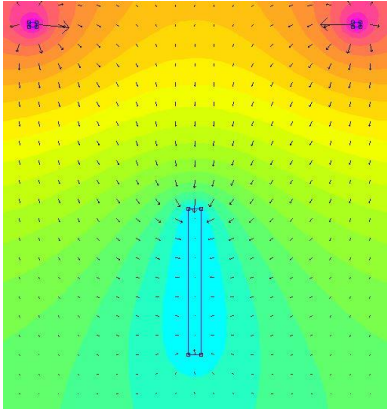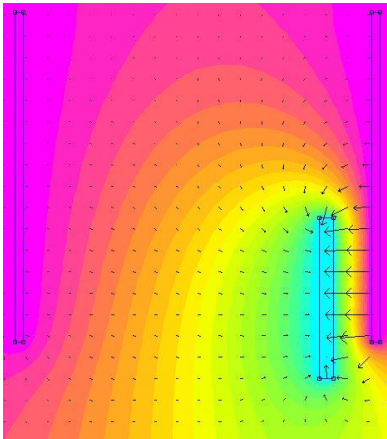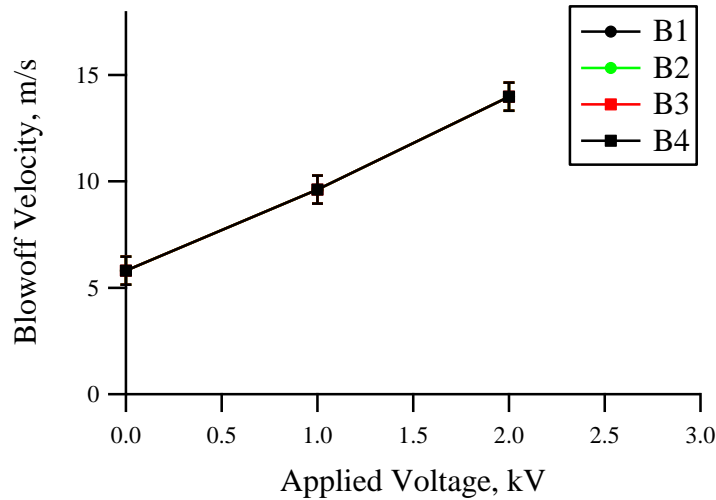
Figure 5. Blowoff characteristics for a premixed methane-air flame in a multi-element burner.
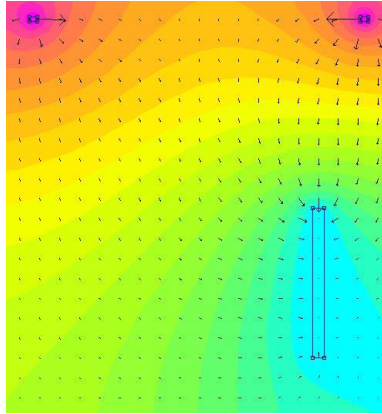
IV. Numerical Results

A 2D model of the potential field produced by the cylinder and ring anode geometries with a grounded burner was simulated with the finite-element modeling tool FEMM. The model does not account for the flame since the program is unable to simulate chemical reactions. Results are shown in Table 3 for an applied voltage of 9 kV. The color contours show the potential distribution while the arrows indicate the electric field streamlines. Longer and larger arrows indicate larger potential gradients and thus stronger electric fields. The electric field lines are generated radially from the anode towards the cathode. A comparison between the single burner at 0 and 60 mm with the cylinder and ring anodes shows that the strength of electric field streamlines produced by the cylinder is significantly higher than the produced by the ring anode, characterized by larger arrows. The larger surface area of the cylinder generates a denser potential field which increases the strength and effectiveness of the electric field in modifying the flame behavior.

A simulation for the multi-element burner showed that the increased cathode surface area caused a shift of the electric field lines and density regions closest to the anode. Though the cathode-anode distance is decreased for burner 4, the voltage drop is still the same, thus stronger local electric fields are generated. It is expected that the burners closest to the anode wall will experience the largest effect of the ionic wind due to the interaction of its flames with this region of higher electric field strength and density. The strong radial component of the field for burner 4 will cause some ions to move radially inward towards burner 3. This would increase the electric forcing effect on burner 3, which would explain why burner 3 had a lower lean limit than the rest as seen in Fig. 5. In this case, burner 3's flame is affected not only by collisions with its own flame ions, but also some of burner 4's ions.
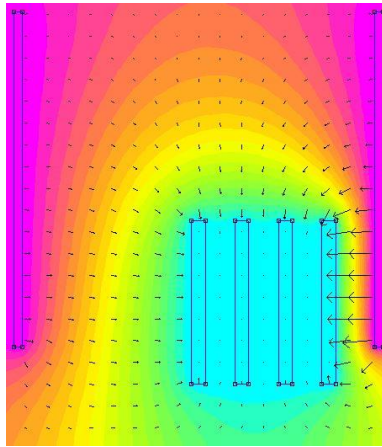
Table 3 Electric field model for different anode geometries and burner configurations.

Burner/Anode Configuration	Model	$\vec{E}$, V/m
(a) Single burner/ Cylinder anode		
(b) Single burner/ Ring anode		
(c) Single burner 60 mm offset/ Cylinder anode		

(d) Single burner 60 mm offset/
Ring anode

(e) 4 burners/
Cylinder anode

V.   Discussion

A.   Lean Flammability Limit

As shown in Fig. 2(a) for the cylinder, an applied electric field caused an extension in the lean flammability limit from $\Phi=0.87$ at 0 kV to $\Phi=0.65$ at 5 kV independently of the radial location of the burner. Increasing the applied voltage had no further effect on the lean limit, indicating that beyond $\Phi=0.65$ the methane concentration is too low to sustain combustion even with the cylinder anode at applied voltages up to 9 kV. A similar behavior was seen with the ring anode as seen in Fig. 2(b). However, higher applied voltages were necessary to reach the same $\Phi=0.65$ lean limit seen with the cylinder, which makes the ring less effective in changing the lean flammability limit. Also, with the ring the flame lean flammability limit showed a dependency on the radial position of the burner.

As seen in Table 3(a-d), the cylinder produces larger potential gradients than the ring at both the center and 60 mm positions, which translates into stronger electric fields. The surface area of the anode was determined as the driving parameter in producing more field lines and higher field densities, and consequently, a good indicator of the electric field strength in a system for a specific anode geometry. Lawton and Weinberg[16] have shown that stronger fields cause higher ionic wind velocities which makes the cylinder anode more effective in enhancing flame stability by causing a larger extension of the lean limit for a given voltage. The ionic wind momentum transfer explains the extension of the lean flammability limit. An applied electric field drives electrons to the anode and high energy ions

to the cathode causing preheating of the fresh gas mixture. The energy provided by the ion collisions reduces the oxidation reaction activation barrier required for sustained combustion beyond the lean flammability limit as seen in Figure 2 and 3.

The fact the lean limit changes with radial location for the ring but not the cylinder anode is due to the increased anode surface area of the cylinder creating a stronger and more uniform field. The cylinder's large potential gradient reaches the maximum lean limit extension at lower voltages such that burner location has no influence. For the ring, the lower potential gradient, thus field strength, means higher voltages are needed to reach the maximum lean limit. Additionally, moving the burner radially closer to the ring increases the electric field strength and allows a lower lean limit for a given voltage. Both the cylinder and ring anodes achieve about the same maximum lean limit of 0.65-0.68, but for the ring this limit occurs at 9 kV and for the cylinder only at 5 kV.

The multi-element burner configuration was only tested with the cylindrical anode since it was found to be more effective than the ring. Figure 3 shows that increasing the applied voltage allows combustion to be sustained at lower mixture ratios. Differently from the single burner with the cylindrical anode configuration, the flames in the multi-element burner extinguished at different ratios, with the burners closest to the cylinder wall having the largest decrease in the lean limits. From Table 3(b), the field lines in the single centered burner in the cylinder configuration are uniform in size. As the burner is moved closer to the cylinder wall however, the lines become non-uniform in size, and thus strength. They become stronger on the right side closest to the wall and weaker on the left size. Thus the different burner exhibit different responses. However, because an electric field is conservative, integrating the electric field around the entire cylinder for a single burner would produce a net electric field strength that is unchanging independent of the burner location and thus the same response as seen in Fig. 2(a). This indicates that it is not only location, but also size of the burner/cathode that affects the flame response.

On the other hand, each burner in the multi-element burner configuration experiences different field strengths. It is seen in Table 3(e) that from the center burner to the one closest to the wall the electric field lines become larger, indicating the lowest and highest electric field strength for burners 1 and 4, respectively. Considering the 2D case seen in Table 3, the field lines directed to each burner is primarily dependent on the radial distance of each burner to the cylinder wall; the lines directed to burner 1 originates from the left side of the cylinder at a distance equal to the radius of the cylinder, while the field lines directed to burner 4 originates at a distance of only 20 mm. This is in accordance with the results seen in Fig. 3.

B.   Blowoff Velocity

Figures 4 and 5 show the effect an applied electric field has on the blowoff velocity limits for the single and multi-element burner cases. Similar to the results of the lean flammability limit, it was noted that the ring anode had a smaller effect on the flame response compared to the cylinder anode, which resulted in a less significant increase in the blowoff velocity and consequently a smaller enhancement in flame stability. As discussed above and seen in Figure 4, the cylinder surface area produces larger potential gradients and electric field lines directed to the flame which increases the strength and action of the electric field on the flame response and thus on the blowoff velocity.

The curves from Figure 4 show that the flame blowoff velocity was dependent on the radial location of the burner for both the cylinder and ring anodes. In the lean flammability limit results, Figure 2, only the flames in the

ring configuration were sensitive to the burner radial position. We did not appear to reach a limit on the blowoff velocity as a function of the burner radial location or applied voltage - the blowoff velocity could be further increased with higher voltages. Moving the burner closer to the anode wall enhanced the effect on blowoff by increasing the field strength and thus ion acceleration and momentum transfer. Contrary to the flammability limit results, the limiting parameter in this case was the applied voltage.

As seen in Figure 5 for the multi-element burner, the blowoff velocity is not dependent on the burner radial location since all flames extinguish at the same flow velocities. The only dependency in this case is on the voltage applied. A comparison between Figure 4(a) and 5 shows the flame blowoff velocity was increased by a factor of 3.36 for the single burner case at 60 mm and 5 kV and by a factor of 1.66 and 2.41 for the multi-element burner case at 1 and 2 kV, respectively. Taken as a ratio, the single burner blowoff velocity increased by a factor of 1.4 ms^{-1}/kV and the multi-element burner by a factor of 4 ms^{-1}/kV. It is important to note that there was no indication that 2 kV is the maximum possible applied voltage that will increase the blowoff velocity in the multi-element burner. We were limited by the flow rate capability of the mass flow controller. Besides showing a higher velocity/voltage factor, the multi-element burner blowoff velocity baseline (0 kV) was already twice as high as the single burner baseline conditions. This indicates the presence of other mechanisms acting in favor of increasing the blowoff condition and eliminating the radial burner location dependency in the multi-element burner configuration that was observed for the single burner case.

One main cause of the lack of radial dependency in the multi-element burner configuration is the proximity of the burners to each other. The heat release from each individual flame provides thermal energy to the adjacent flames by convection and radiation. The mutual heat transfer allows the flames to sustain each other's combustion process by increasing the temperature and thus flame speed, and providing a secondary heat source to preheat the reactants. The net result is a higher blowoff velocity with and without an applied voltage. As one or more of the burners go out due to the flame speed not being able to match that of the incoming gas, the overall thermal energy of the system decreases. At this point, the mutual heat transfer between the burners decreases which causes a decrease of the flame speed in the remaining burners followed by blow out. On the other hand, the single burners are surrounded by ambient air so heat release is quickly dissipated to the surroundings. Also, the overall flame surface area in the multi-element burner configuration is larger due to multiple flames and higher flow velocities, which increases the number of ions and electrons inside of the cylinder. Since the effects of the ionic wind are caused by ionic momentum transfer, a higher ion density will lead to more significant flame responses.

Ion collisions can transfer energy into both translation and internal energy modes of fuel and air molecules. Energy into translation will affect the bulk flow velocity, which is related to blowoff, while internal energy affects reaction rates which are related to the lean flammability limit. The lack of a blowoff limit at the same voltage as the lean limit indicates the ionic wind is more effective in retarding the neutral flow velocity that preheats the reactants. This is logical given the similar masses of flame ions (HCO^+ and H_3O^+) and fuel and air molecules that preferentially transfer energy into translation. Collisions with electrons or very high energy particles will preferentially transfer energy into internal modes. However, in this case the electrons are accelerated downstream and thus have limited interaction with the incoming reactants.

VI.   Conclusions

In this work the effect of an electric field on the response of an atmospheric, premixed methane-air flame was compared for two burner configurations using two anode geometries. The flame response was quantified by measuring the changes in the flame lean flammability limit and blowoff velocity. The burners consisted of single and multi-element configurations to determine the difference between element radial location and flame-to-flame contact interaction as an atmospheric analogy to the functionality of a liquid propellant rocket engine injector. Flame lean limit of flammability and blowoff velocity was determined for each burner configuration and electrode geometry at different applied voltages.

The electric field induced ionic wind causes mass transfer of ions in the field direction. Energetic ions directed towards the burners preheat the fresh gas mixture, leading to an increase in the flame temperature and speed. The observed results showed an extension of the lean flammability limit of the flame from an equivalence ratio of 0.86 to 0.65. The blowoff velocity was increased from ~2.90 m/s to a maximum of ~10 m/s for the single burner and from ~5.8 m/s to 14 m/s for the multi-element burner. Overall, single burners closer to the anode wall had a more significant effect on the flame response than burners centered in the anode, thus stronger effect on the flammability limit and blowoff velocity. Stronger electric fields are generated at those locations since it is a function of the distance between the anode and cathode. The higher initial blowoff velocity for the multi-element burner was caused by a higher heat release from the presence of multiple flames which enabled sustained combustion at higher flow rates. The cylinder anode had a stronger effect on both the flammability limit and blowoff velocity for a given voltage due to larger surface area leading to higher field strengths.

It has been concluded that the multi-element burner and cylinder configuration was the most effective configuration tested. The multi-element burner increases the combustion efficiency by increasing heat release and decreasing losses to the surroundings, and the large surface area of the cylinder provides a more efficient field distribution. This combination enhances combustion stability and reduces the voltage requirements to produce desirable flame responses.

The presence of multiple flames in a system enhances the effects of the applied electric field so, theoretically, the techniques described here have the potential to effectively affect the flame response in rocket engine with multiple injection ports. Combustion instability is always an issue in rocket engines, especially during development phases. Although experience has led to several ways to suppress instabilities much is still unknown about the combustion instability process itself. Applying electric fields in the combustion chamber has the potential to suppress these instabilities and provide a method to better understand the coupling mechanisms that lead to instabilities. Future work will focus on studying an active control system with the goal of breaking, or at least damper, the coupling between the combustion process and the acoustic energy in the chamber by interacting with the system combustion dynamics and heat release.

REFERENCES

[1] Brande, W. T., "The Bakerian lecture: On some new electro-chemical phenomena," *Philos. Trans. R. Soc.*, vol. 104, 1814, pp. 51–61.

[2] Bradley, D., and Nasser, S. H., "Electrical coronas and burner flame stability," *Combustion and Flame*, vol. 55, 1984, pp. 53–58.

[3] Jaggers, H., C., and von Engel, A., "The effect of electric fields on the burning velocity of various flames," *Combustion and Flame*, vol. 16, 1971, pp. 275–285.

[4] Calcote, H. F., and Berman, C. H., "Increased methane-air stability limits by a DC electric field," *Proceeding of the ASME Fossil Fuels Combustion Symposium*, 1989, pp. 25–31.

[5] Bak, M. S., Im, S. K., Mungal, M. G., and Cappelli, M. a., "Studies on the stability limit extension of premixed and jet diffusion flames of methane, ethane, and propane using nanosecond repetitive pulsed discharge plasmas," *Combustion and Flame*, vol. 160, 2013, pp. 2396–2403.

[6] Kim, M. K., Chung, S. H., and Kim, H. H., "Effect of AC electric fields on the stabilization of premixed Bunsen flames," *Proceedings of the Combustion Institute*, vol. 33, 2011, pp. 1137–1144.

[7] Ata, a., Cowart, J. S., Vranos, A., and Cetegen, B. M., "Effects of Direct Current Electric Field on the Blowoff Characteristics of Bluff-Body Stabilized Conical Premixed Flames," *Combustion Science and Technology*, vol. 177, 2005, pp. 1291–1304.

[8] Saito, M., Sato, M., and Sawada, K., "Variation of flame shape and soot emission by applying electric field," *Journal of Electrostatics*, vol. 39, 1997, pp. 305–311.

[9] Marcum, S. D., and Ganguly, B. N., "Electric-field-induced flame speed modification," *Combustion and Flame*, vol. 143, 2005, pp. 27–36.

[10] Wisman, D. L., Marcum, S. D., and Ganguly, B. N., "Electrical control of the thermodiffusive instability in premixed propane-air flames," *Combustion and Flame*, vol. 151, 2007, pp. 639–648.

[11] Noorani, R. I., "Effect of Electric Fields on the Blowoff Limits of a Methane Air Flame," *AIAA Journal*, 1985, pp. 1452–1454.

[12] Kuhl, J., Jovicic, G., Zigan, L., Will, S., and Leipertz, A., "Influence of electric fields on premixed laminar flames: Visualization of perturbations and potential for suppression of thermoacoustic oscillations," *Proceedings of the Combustion Institute*, vol. 35, 2015, pp. 3521–3528.

[13] Most, D., Hammer, T., Lins, G., Branston, D. W., Altendorfner, F., Beyrau, F., and Leipertz, A., "Electric Field Effects for Combustion Control - Optimized Geometry," *International Conference on Phenomena in Ionized Gases*, 2007, pp. 1863–1866.

[14] Sakhrieh, A., Lins, G., Dinkelacker, F., Hammer, T., Leipertz, A., and Branston, D. W., "The influence of pressure on the control of premixed turbulent flames using an electric field," *Combustion and Flame*, vol. 143, 2005, pp. 313–322.

[15] Payne, K. G., and Weinberg, F. J., "A preliminary investigation of field-induced ion movement in flame gases and its applications," *Proceedings of the Royal Society*, vol. 250, 1959, pp. 316–336.

[16]   Lawton, J., and Weinberg, F., J., "Maximum ion currents from flames and the maximum practical effects of applied electric fields," *Proceedings of the Royal Society*, vol. 277, 1964, pp. 468–497.

[17]   Kadowaki, S., "The effects of heat loss on the burning velocity of cellular premixed flames generated by hydrodynamic and diffusive-thermal instabilities," *Combustion and Flame*, vol. 143, 2005, pp. 174–182.

[18]   Van Den Boom, J. D. B. J., Konnov, a. a., Verhasselt, a. M. H. H., Kornilov, V. N., De Goey, L. P. H., and Nijmeijer, H., "The effect of a DC electric field on the laminar burning velocity of premixed methane/air flames," *Proceedings of the Combustion Institute*, vol. 32 I, 2009, pp. 1237–1244.

[19]   Wisman, D. L., Ganguly, B. N., and Marcum, S. D., "Importance of Electrode Location on Flames Modified by Low Applied Electric Fields," *46th AIAA Aerospace Sciences Meeting and Exhibit*, 2008, pp. 1–10.

[20]   Turns, S. R., *An Introduction to Combustion: Concepts and Applications*, New York: McGraw-Hill, 2012.

[21]   Law, C. K., and Egolfopoulos, F. N., "A Unified Chain-Thermal Theory of Fundamental Flammability Limits," *Twenty-Fourth Symposium (International) on Combustion*, The Combustion Institute, Pittsburgh, PA: 1973, p. 1119.